Influence of local interstellar medium on cosmic ray properties

Siming Liu, Yiran Zhang, Zhangxi Xue

School of Physical Science and Technology, Southwest Jiaotong University, Chengdu, Sichuan, China

Outline

- A brief review to the cosmic-ray (CR) properties
  - CR spectra
  - Anisotropy observations
  - Compton-Getting (CG) effect
  - Diffuse dipole anisotropy
- Properties of the local interstellar medium and a three component model for CR properties
- Nonuniform convection scenario
  - Large-scale anisotropies from regular fluid nonuniformity
  - Small-scale anisotropies from turbulent convection
- Conclusions

CR Spectra

- Relativistic high-energy particles
  - p ~ 90%, He ~ 9%, e^- ~ 1%
  - Energy density ~ eV/cm^3
- Power-law spectrum
  - Energy spectral index ~ 2.7
  - Maximum energy ~ 50 EeV
- High level of isotropy
  - Relative anisotropy ~ 0.1%
  - Implication: Diffusive propagation

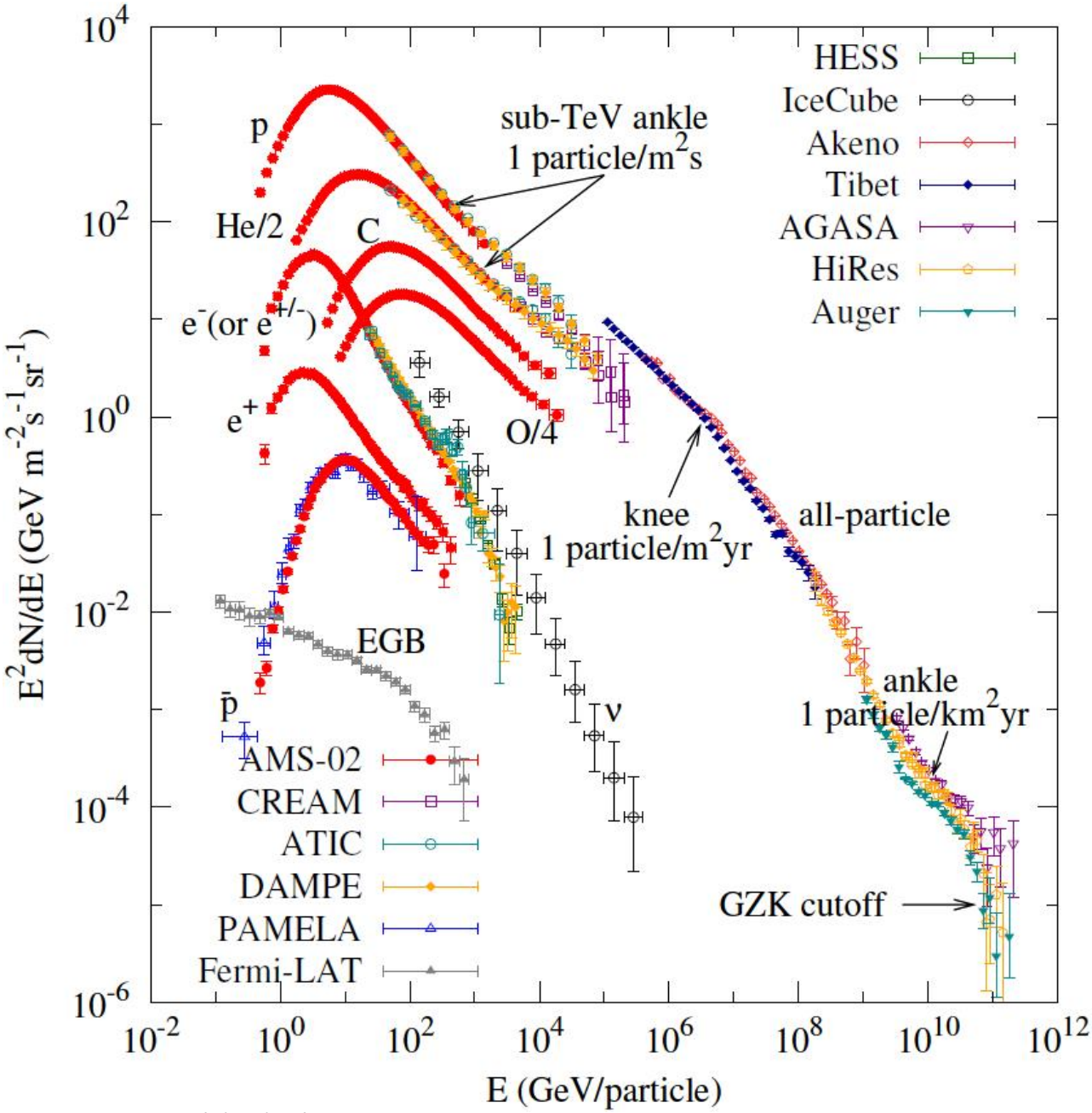

LHAASO 2022 CPC

Anisotropy Observations

- CR intensity sky
  - Dipole signals dominate

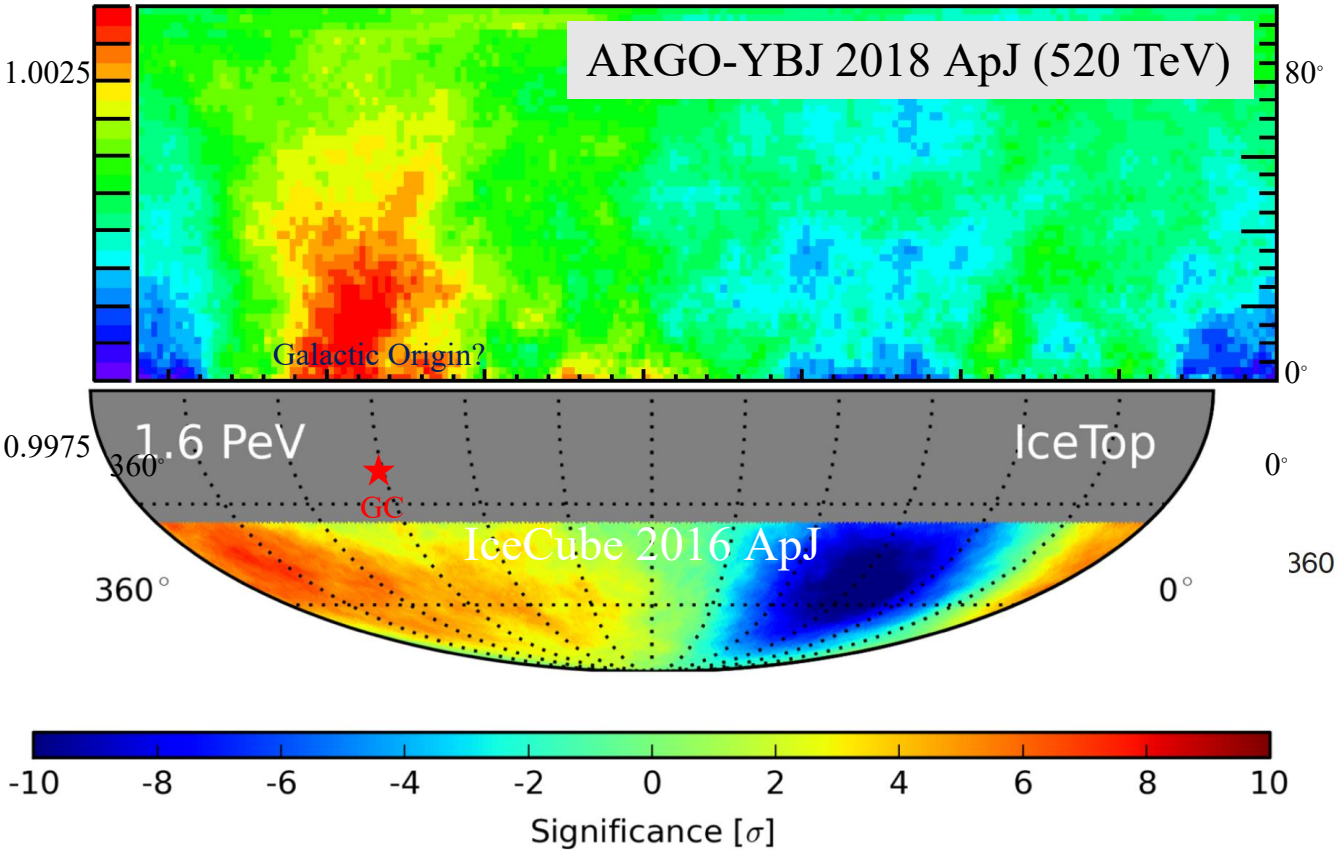

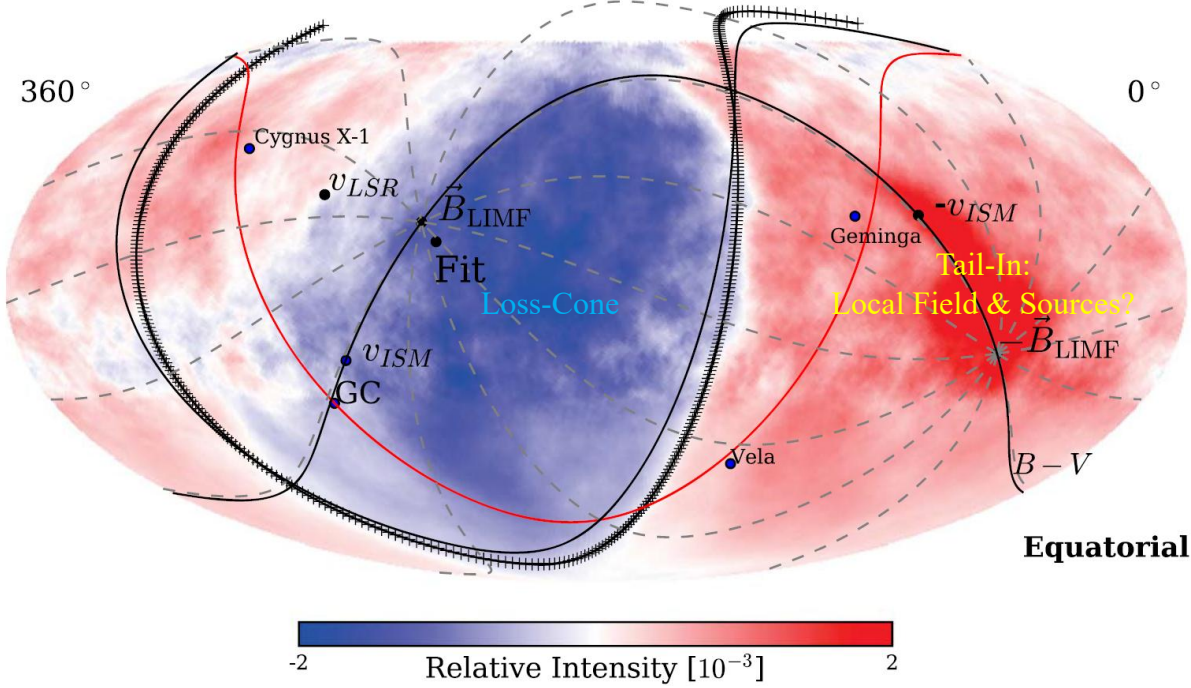

HAWC & IceCube 2019 ApJ, 871 (10 TeV)

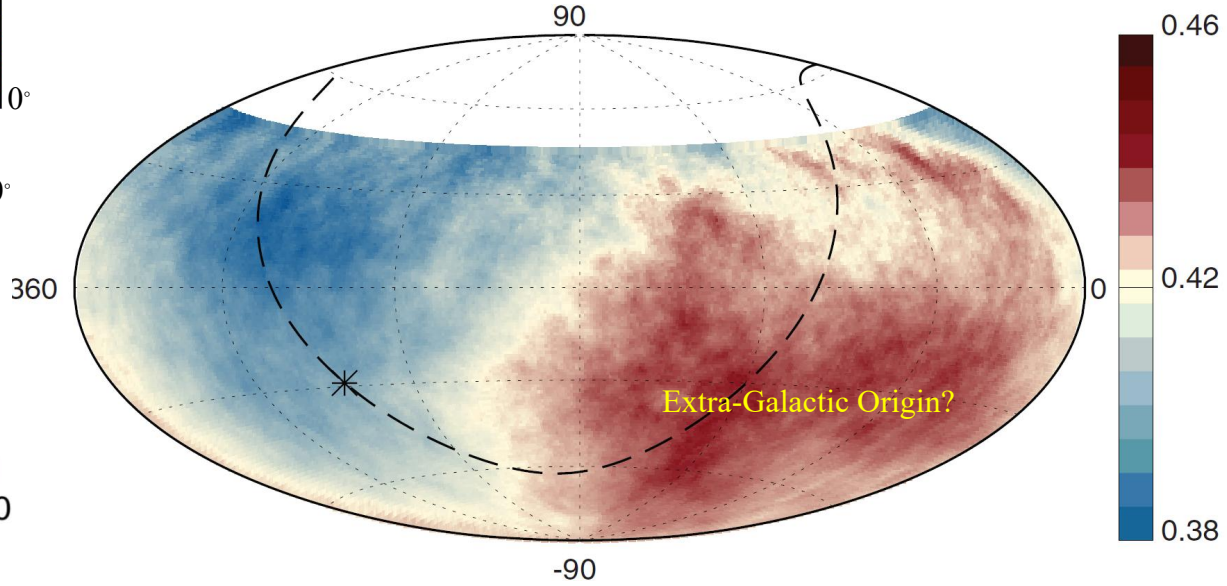

Auger 2017 Science (above 8 EeV)

Dipole Anisotropy

- Energy-dependent CR dipole anisotropy
  - The amplitude roughly increases with energy
  - Anomalous signals: 10-100 TeV & 0.1-10 Ee
    - Amplitude decrease
    - Phase flip

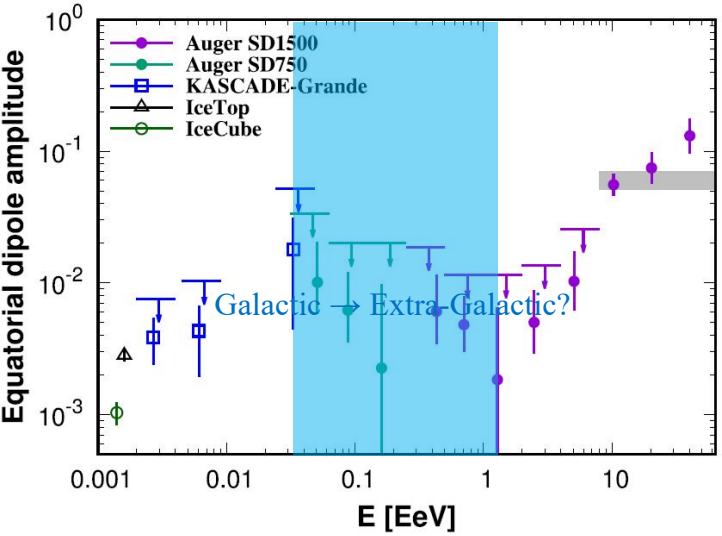

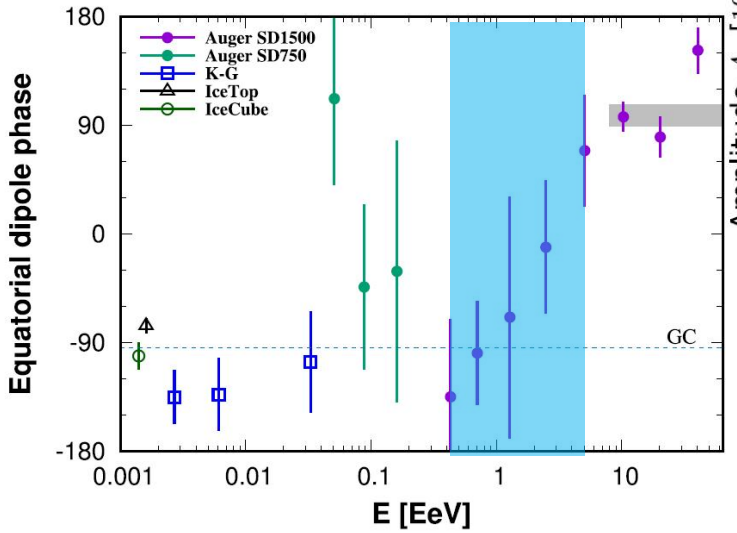

Pierre Auger Observatory 2020 ApJ

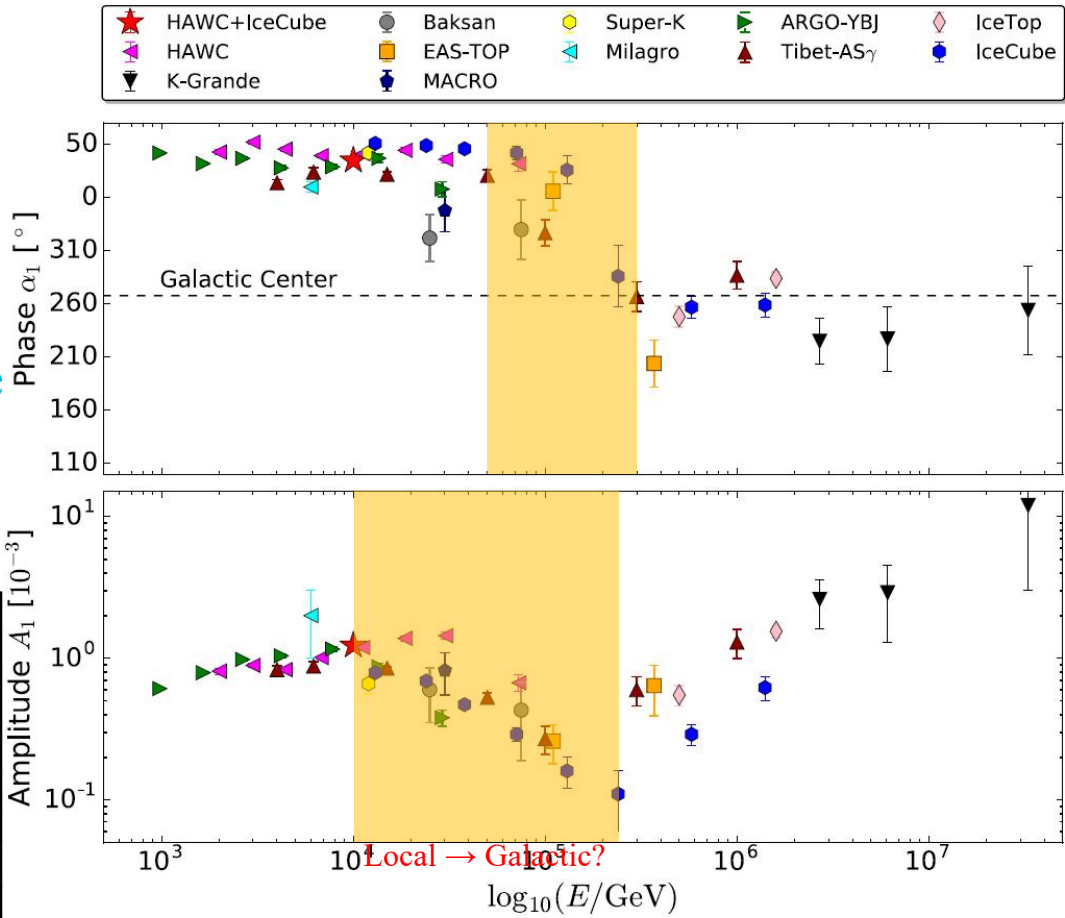

HAWC & IceCube 2019 ApJ

Anisotropy Observations

- CR small-scale anisotropies
  - TeV angular power spectrum $\propto \ell^{-3}$ ($\ell_{\text{dipole}} = 1$, $\ell_{\text{quadrupole}} = 2$...)
  - No statistically significant small-scale anisotropy has been observed above PeV energies

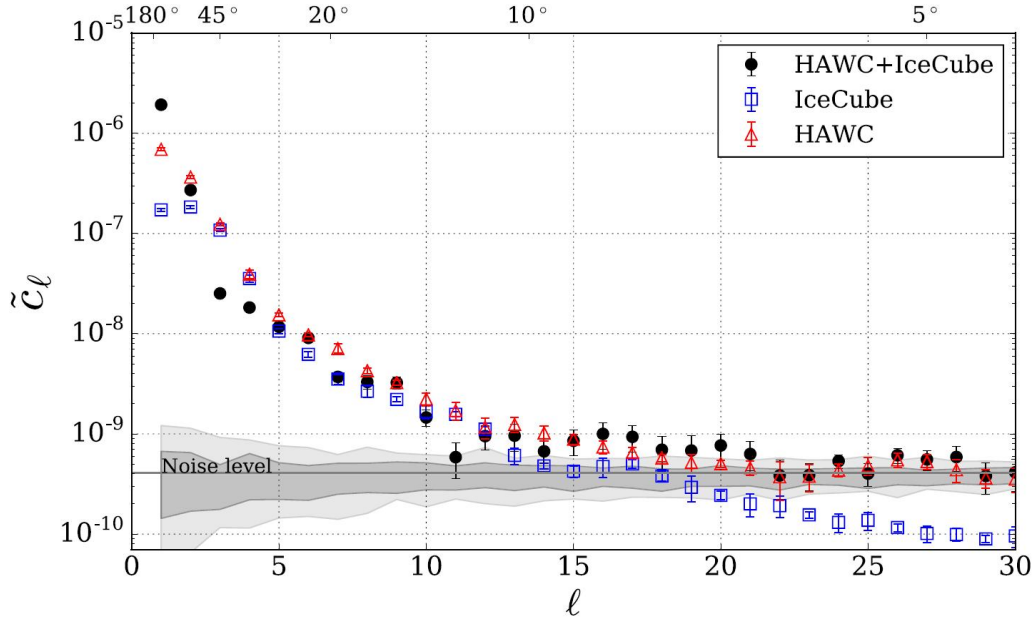

HAWC & IceCube 2019 ApJ (10 TeV)

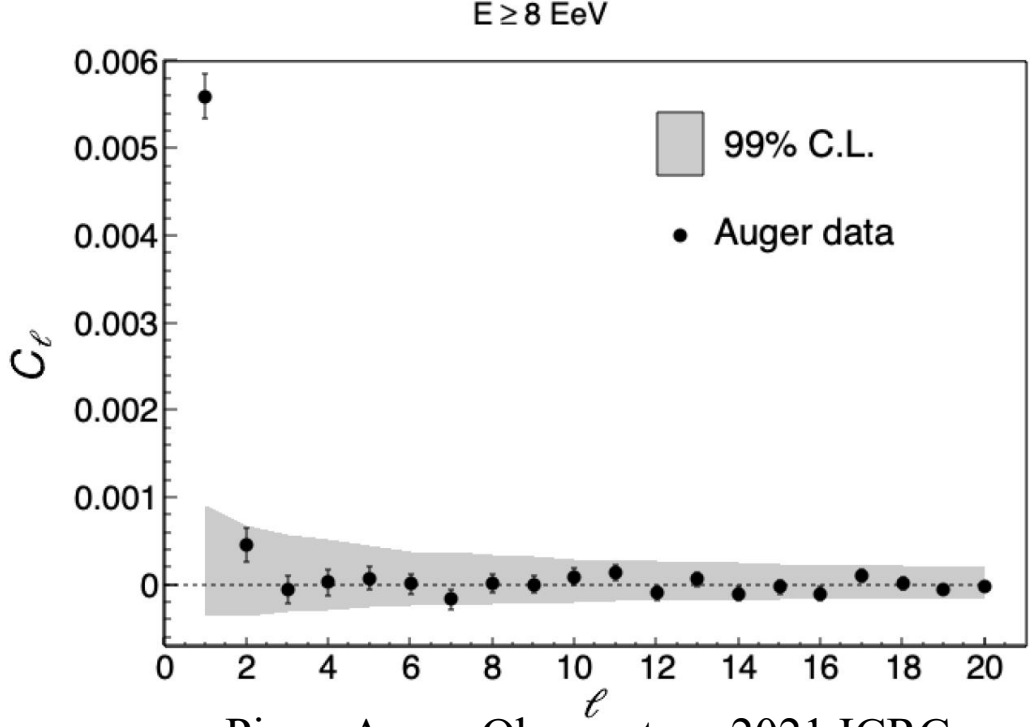

Pierre Auger Observatory 2021 ICRC

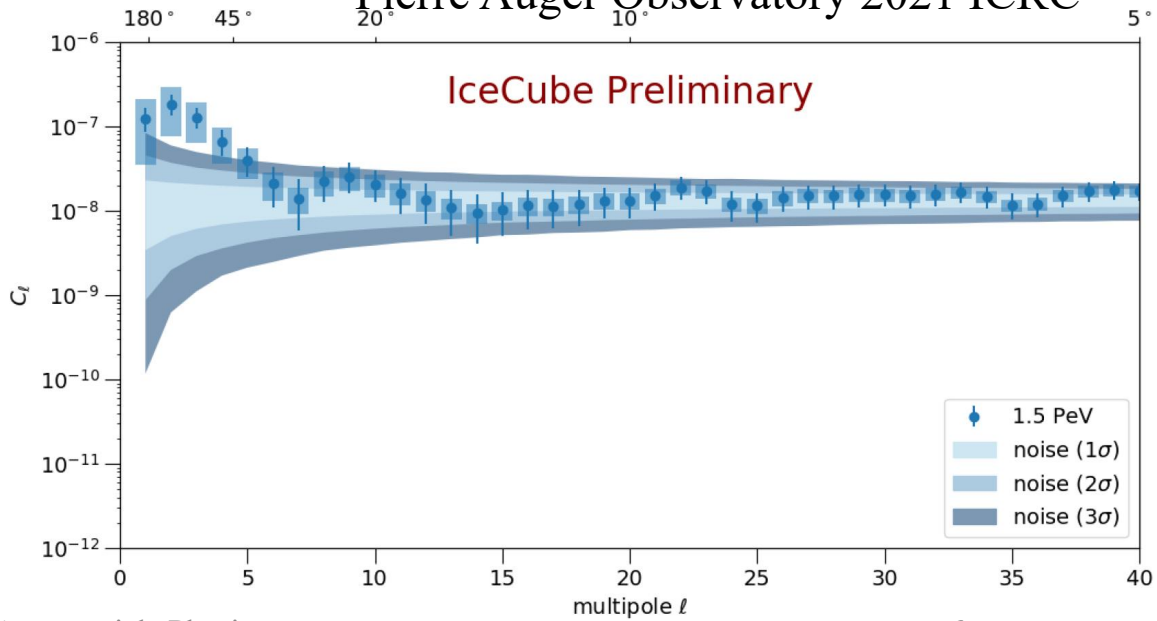

IceCube 2023 ICRC

CG Effect

- Original version: Compton & Getting 1935 Physical Review
- Convectional anisotropy
  - Uniform convection (i.e., the Doppler effect) of particles can produce a dipole anisotropy

$$\Delta_{\mathrm{CG}} f = (-\boldsymbol{P} \cdot \boldsymbol{u}/V)\, \partial f / \partial P$$

  - CRs (energy spectral index ~ 2.7) without corotation with Galaxy would have an energy-independent dipole anisotropy ~ 0.2% observed at Earth (Galactic rotation speed ~ 220 km/s), which is inconsistent with CR observations
  - Insignificant CG effect: The rest frame of CRs is close to the local standard of rest

Diffuse Dipole Anisotropy

- Classical diffusion approximation
  - In the scattering time, particles tend to completely lose information about their initial states
  - Fluctuation-relaxation equilibrium: The diffuse anisotropy can be understood via backtracking particle trajectories within the mean free path $\boldsymbol{\lambda}$, leading (only) to a dipole moment

$$\Delta_{\text{diffuse}} f = -\boldsymbol{\lambda} \cdot \nabla f$$

- The energy-dependent CR anisotropy can be modeled with the diffuse picture, as the mean free path typically increases with energy
  - The diffuse anisotropy is also affected by the source distribution
  - TeV CR spectral and dipole anisotropy anomalies: Nearby source model (e.g., Ahlers 2016 PRL, Liu et al. 2017 PRD, Qiao et al. 2019 JCAP, Zhao et al. 2022, ApJ, Zhang et al. 2022 MNRAS)

Properties of local interstellar medium

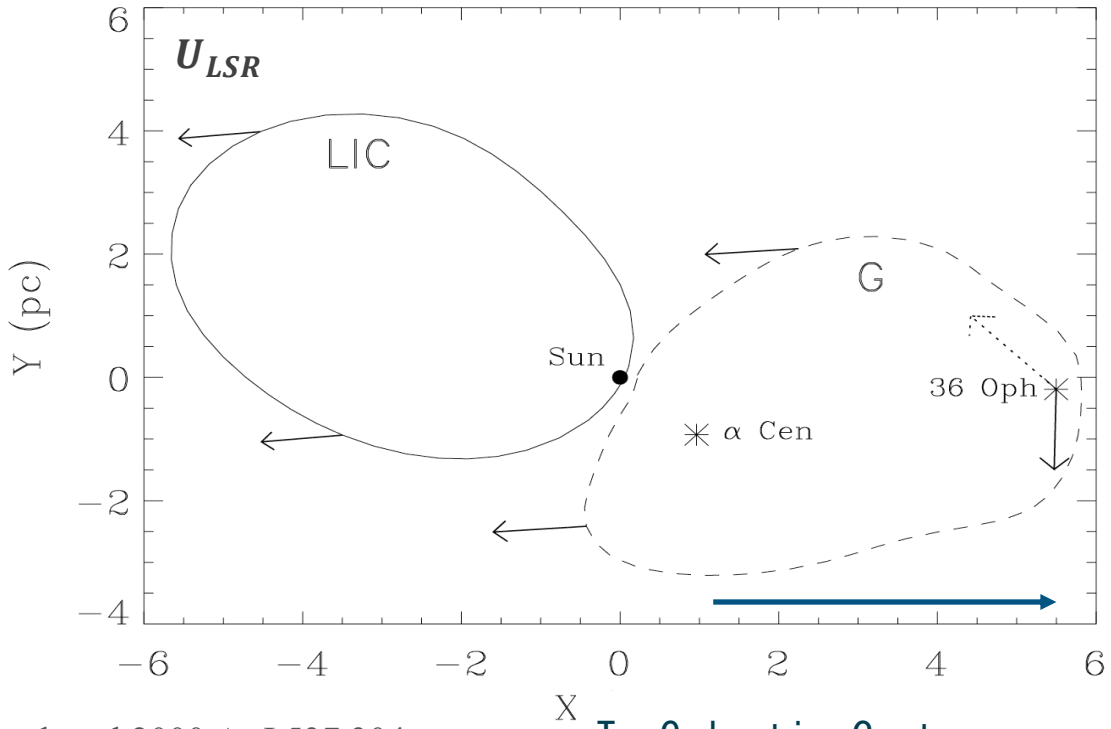

Wood et al 2000 ApJ 537 304

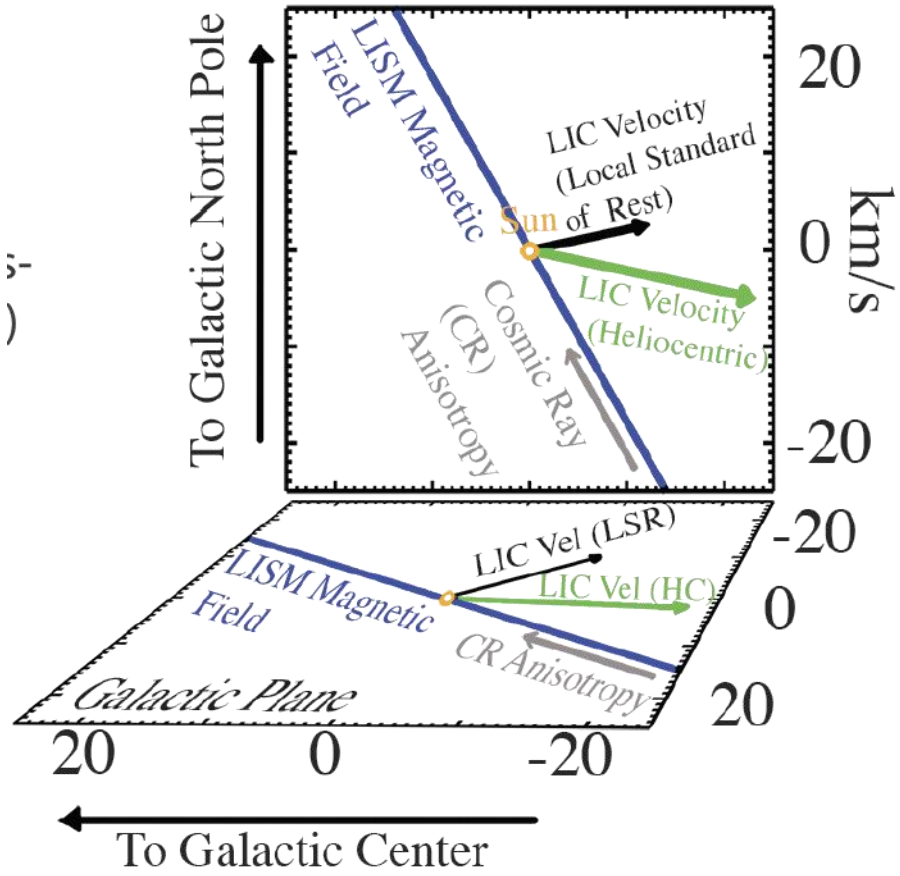

Schwadron, N. A. et al 2014 Science 343 988

Velocity of the Local Interstellar Cloud (LIC) in the Heliocentric frame:

$$U_{HC} = 23.2 km/s$$

Velocity of LIC in the Local Standard of Rest:

$$U_{LSR} = 15.6 km/s$$

The angle between LISM and U_{LSR}: $\theta = 87.6°$

A Three Component Model: Spectrum

$$J_{\rm b}(R) = \frac{v\ w\ H_G^2}{4\pi V_G D(R)} \times Q_{0\rm b} \left(\frac{R}{\rm GV}\right)^{-\Gamma} \exp\left(-\frac{R}{R_{\rm cut}}\right),$$

$$J_{\rm n}(R) = \frac{c}{4\pi} \exp\left(-\frac{u_{\rm LSR}}{\kappa_{xx}} x\right) \frac{Q_{\rm n}(R)}{(4\pi T_{\rm n})^{3/2} D_{\parallel}(R)^{1/2} D_{\perp}(R)} \times \exp\left(-\frac{r_{\parallel}^2}{4D_{\parallel}(R)T_{\rm n}} - \frac{r_{\perp}^2}{4D_{\perp}(R)T_{\rm n}}\right), \quad (6)$$

where

$$\kappa_{xx} = \kappa_{\parallel} \cos^2\theta + \kappa_{\perp} \sin^2\theta \quad (7)$$

$$J_{\rm c}(R) = \frac{c}{4\pi} Q_{\rm c}(R) \times [4\pi T_{\rm c} \cdot D(R)]^{-3/2} \exp\left[-\frac{r_{\rm c}^2}{4D(R)T_{\rm c}}\right],$$

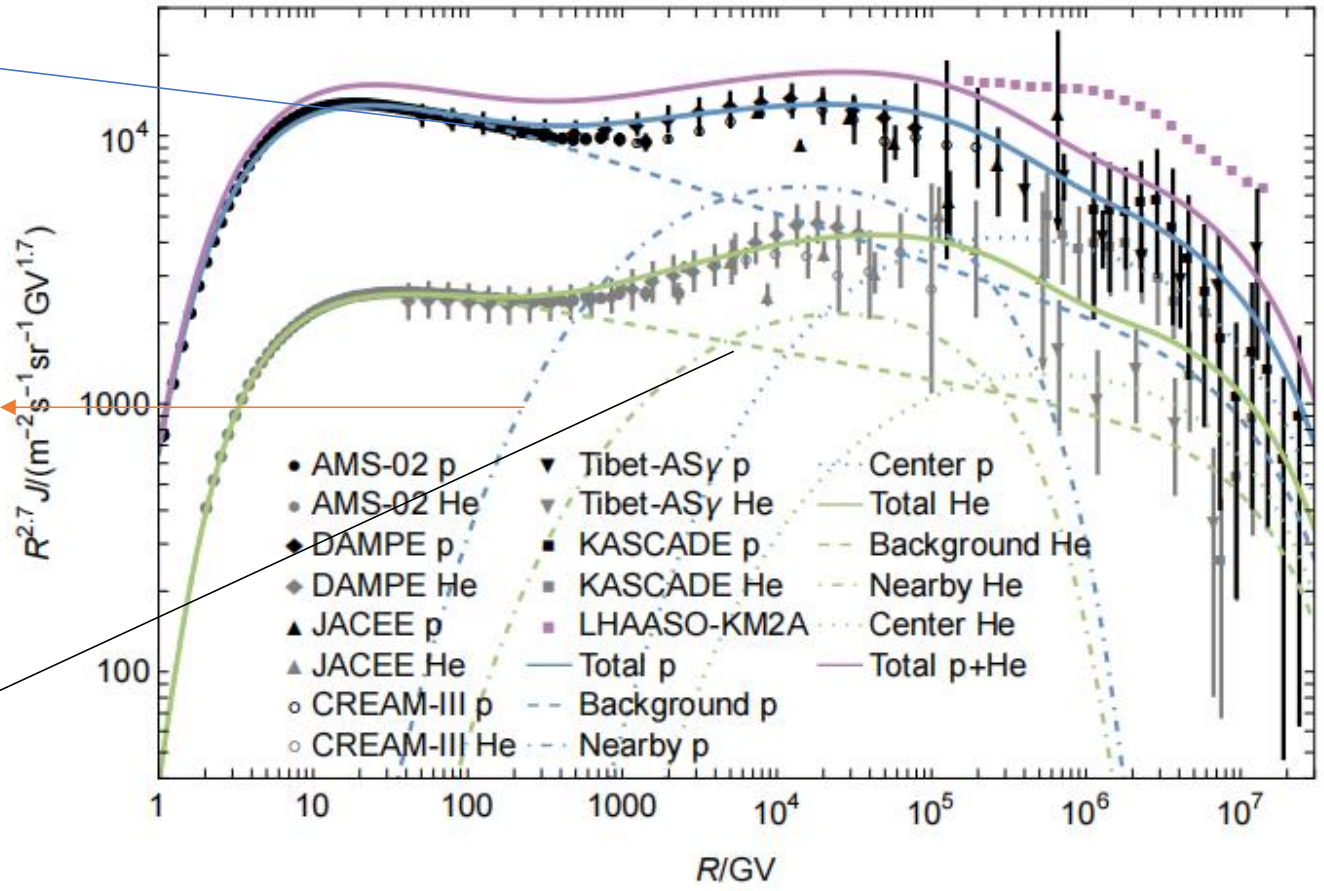

Zhang et al. 2022 MNRAS, 511

A Three Component Model: Anisotropy

TABLE I. The best-fitting parameters of the model.

Parameters[a]	Best-fitted	Unit
$Q_{0\mathrm{b,p}}$	1.75×10^{52}	GV^{-1}
$Q_{0\mathrm{b,He}}$	2.65×10^{51}	GV^{-1}
$Q_{0\mathrm{n,p}}$	1.2×10^{53}	GV^{-1}
$Q_{0\mathrm{n,He}}$	2×10^{52}	GV^{-1}
$Q_{0\mathrm{c,p}}$	7×10^{57}	GV^{-1}
$Q_{0\mathrm{c,He}}$	8×10^{56}	GV^{-1}
R_{cut}	20	PeV
R_{cutn}	0.4	PeV
ϕ	0.89	GV
D_0	1×10^{28}	$\mathrm{cm}^2\ \mathrm{s}^{-1}$
Γ_{p}	2.55	

[a] Subscripts p and He stands for proton and helium respectively.

$$\boldsymbol{\xi} = \frac{3}{v} C \boldsymbol{u}_{\mathbf{HC}} + \frac{J_{\mathrm{n}}}{J_{\mathrm{n}} + J_{\mathrm{b}} + J_{\mathrm{c}}} \boldsymbol{\xi}_{\mathbf{n}} + \frac{J_{\mathrm{b}}}{J_{\mathrm{n}} + J_{\mathrm{b}} + J_{\mathrm{c}}} \boldsymbol{\xi}_{\mathbf{b}} + \frac{J_{\mathrm{c}}}{J_{\mathrm{n}} + J_{\mathrm{b}} + J_{\mathrm{c}}} \boldsymbol{\xi}_{\mathbf{c}}$$

$$\boldsymbol{\xi}_{\mathbf{b}} = \delta_{\mathrm{b}} \cos\theta_{\mathrm{b}} \hat{\boldsymbol{b}},$$

$$\boldsymbol{\xi}_{\mathbf{c}} = \delta_{\mathrm{c}} \cos\theta_{\mathrm{c}} \hat{\boldsymbol{b}},$$

$$\boldsymbol{\xi}_{\mathbf{n}} = -\frac{3}{v} \left(\frac{\kappa_{\parallel}}{\kappa_{xx}} u_{\mathrm{LSR}} \cos\theta \hat{\boldsymbol{b}} + \frac{\kappa_{\perp}}{\kappa_{xx}} u_{\mathrm{LSR}} \sin\theta \hat{\boldsymbol{e}}_{\perp \mathbf{1,n}} \right),$$

$$\kappa_{\perp} = \kappa_{\parallel} / [1 + (\omega\tau)^2]$$

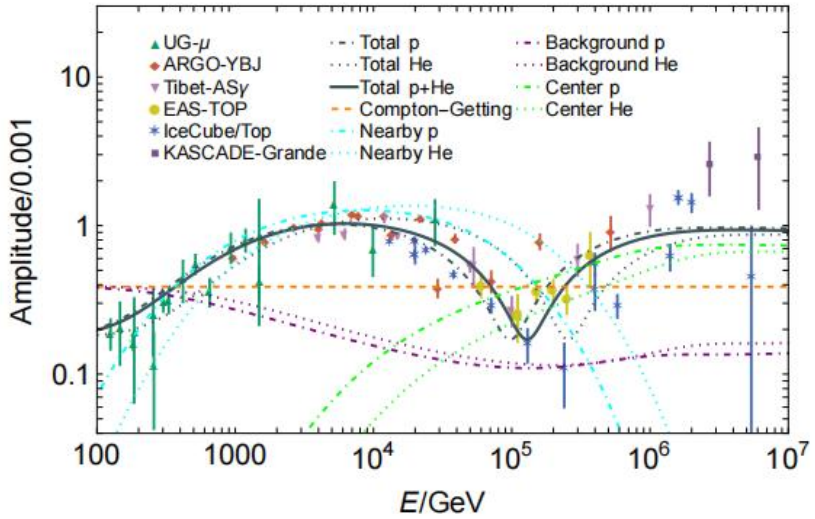

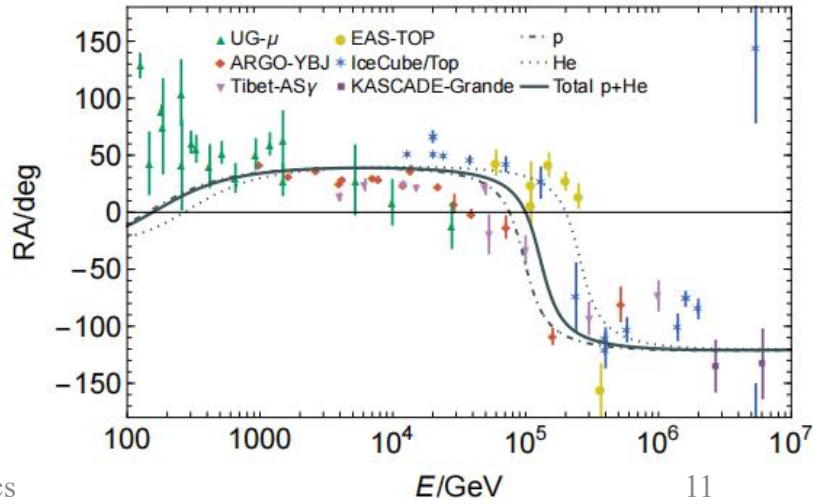

Dependence of the Anisotropy on U_{LSR}

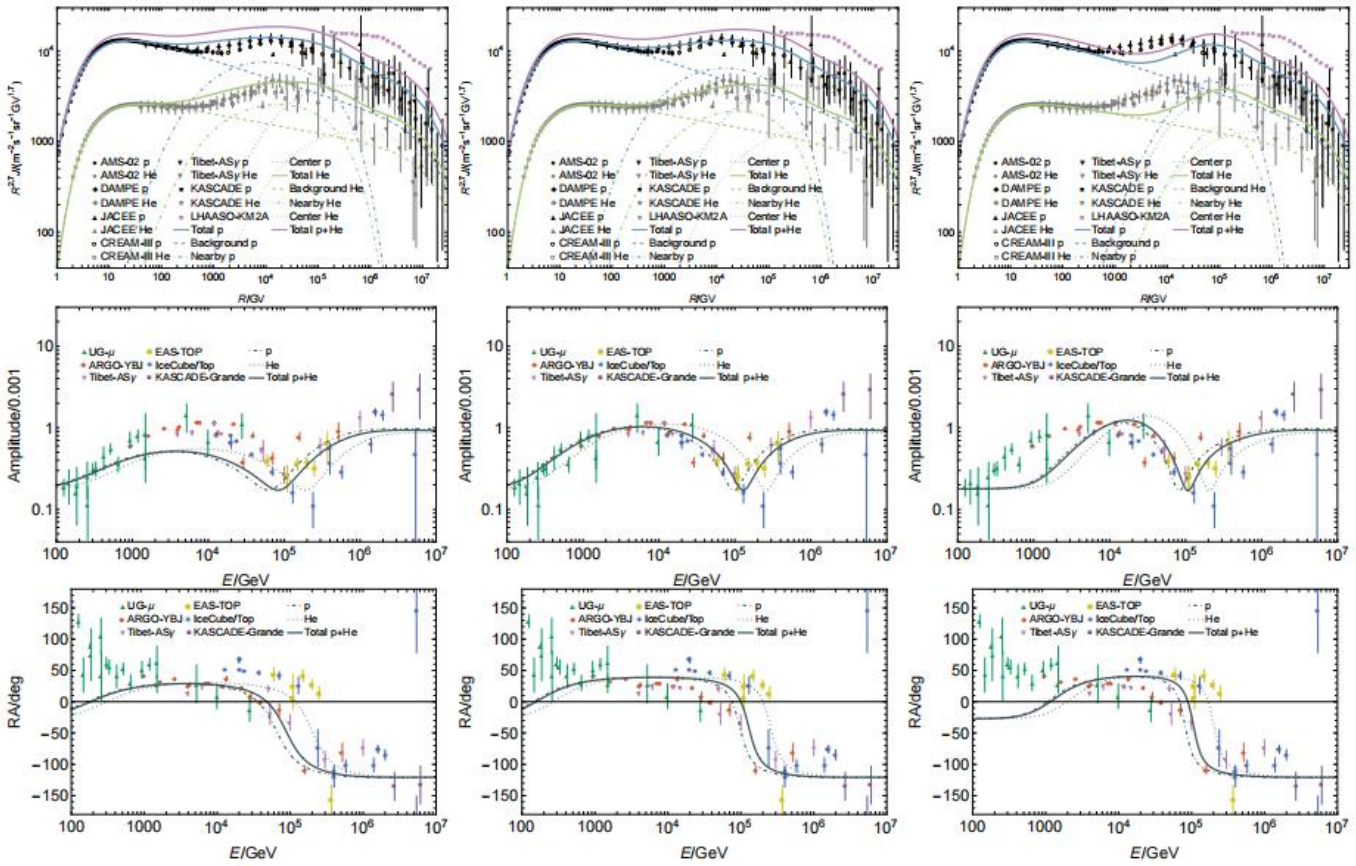

FIG. 2. Influences of $V_\odot$ on fitting results. Left column: Fitting results of $V_\odot = 14$ km s^{-1}. Middle column: The best-fitting results where $V_\odot = 17$ km s^{-1}. Right column: Fitting results of $V_\odot = 20$ km s^{-1}.

Dependence of the Anisotropy on U_{HC}

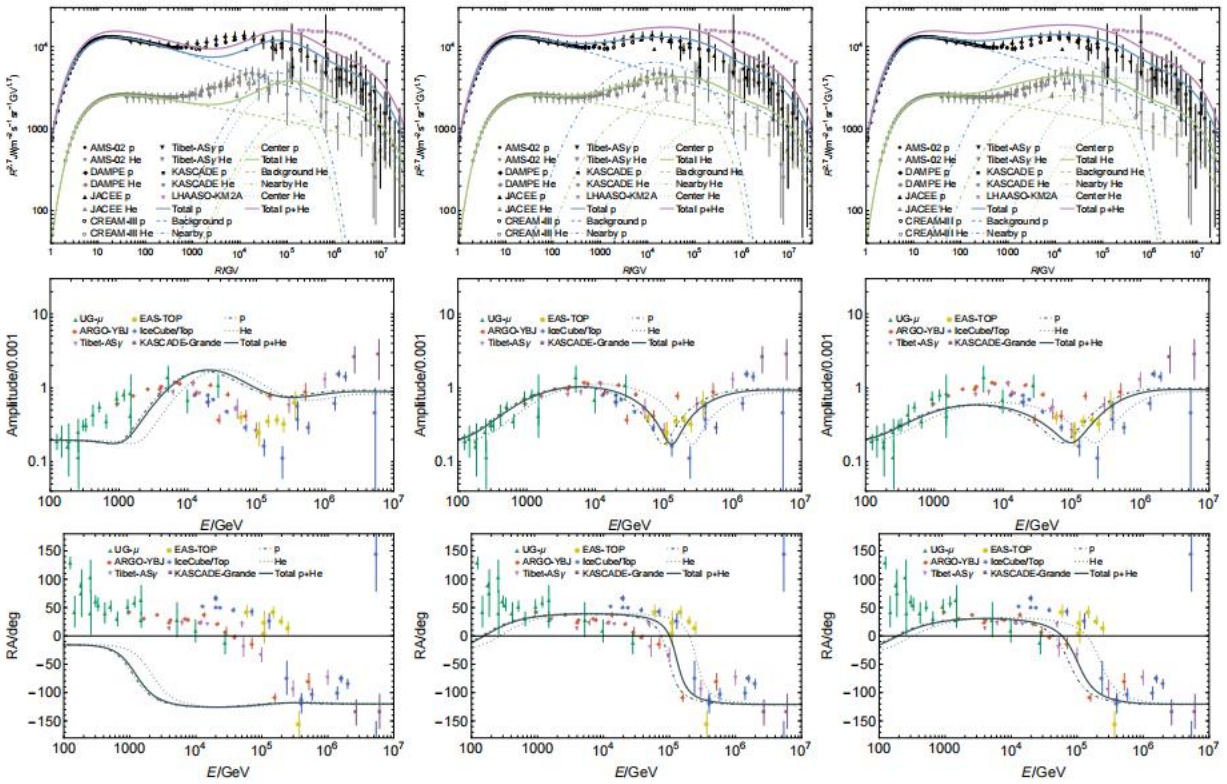

FIG. 4. Influences of $\boldsymbol{u_{HC}}$ on fitting results. Left column: Fitting results of $u_{HC} = 23.2$ km/s with a right ascension of 78.5° and a declination of 18.0° [1]. Middle column: The best-fitting results where $u_{HC} = 25.4$ km/s with a right ascension of 74.9° and a declination of 17.6° [2]. Right column: Fitting results of $u_{HC} = 26.6$ km/s with a right ascension of 75.0° and a declination of 17.7° [3].

[1] N. Schwadron, F. Adams, E. Christian, P. Desiati, P. Frisch, H. Funsten, J. Jokipii, D. McComas, E. Moebius, and G. Zank, Science **343**, 988 (2014).

[2] N. Schwadron, E. Möbius, T. Leonard, S. Fuselier, D. McComas, D. Heirtzler, H. Kucharek, F. Rahmanifard, M. Bzowski, M. Kubiak, *et al.*, The Astrophysical Journal Supplement Series **220**, 25 (2015).

[3] P. Swaczyna, M. Bzowski, J. Heerikhuisen, M. Kubiak, F. Rahmanifard, E. Zirnstein, S. Fuselier, A. Galli, D. McComas, E. Möbius, *et al.*, The Astrophysical Journal **953**, 107 (2023).

Dependence of the Anisotropy on Local Turbulence

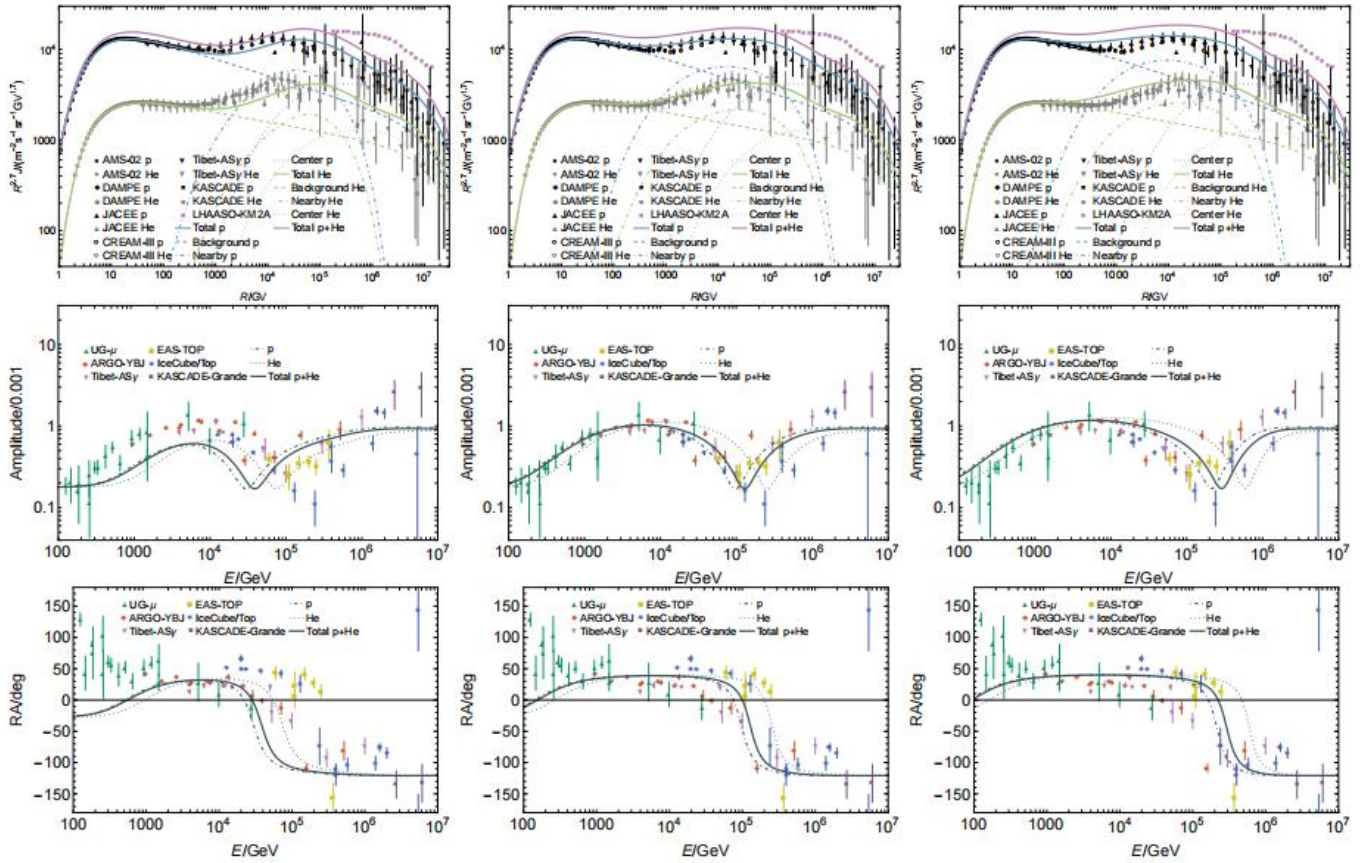

FIG. 5. Influences of $E_{\rm cr}$ on fitting results. Left column: Fitting results of $E_{\rm cr} = 1$ PeV. Middle column: The best-fitting results where $E_{\rm cr} = 6$ PeV. Right column: Fitting results of $E_{\rm cr} = 40$ PeV.

Large-Scale Anisotropies from Regular Fluid Nonuniformity

- Conventional point of view: The energy-dependent CR anisotropy is dominated by the diffuse term with a minor convection (CG) effect
- Can convection have effects producing energy-dependent anisotropies?
  - Earl et al. 1988 ApJL studied CR viscosity with the classical diffusion approximation (Bhatnagar-Gross-Krook analysis); their derivation of the transport equation under nonuniform convection has an intermediate step concerning the distributional fluctuation

Scattering Time

$$f_1 \approx \tau\left[-\frac{p_i}{m}\frac{\partial f_0}{\partial x_i} + mU_j\frac{\partial U_i}{\partial x_j}\frac{p_i}{p}\frac{\partial f_0}{\partial p}\right.$$

Diffuse Dipole

Inertial Dipole $\propto d\boldsymbol{U}/dt = \partial\boldsymbol{U}/\partial t + \boldsymbol{U}\cdot\nabla\boldsymbol{U}$

$$\left. + p_j\frac{\partial U_i}{\partial x_j}\frac{p_i}{p}\frac{\partial f_0}{\partial p} - \frac{\partial U_i}{\partial x_j}\frac{\langle p_i p_j\rangle}{p}\frac{\partial f_0}{\partial p}\right]$$

Shear Quadrupole $\propto S_{ij} = (\partial U_j/\partial x_i + \partial U_i/\partial x_j)/2 - \delta_{ij}\nabla\cdot\boldsymbol{U}/3$

Large-Scale Anisotropies from Regular Fluid Nonuniformity

- Convection-diffusion approximation
  - Complete relaxation of particle trajectories can be observed only in the rest frame of the scattering center
  - Nonuniform convection: Scattering centers at different locations have relative motion, leading to inertial and shear forces ($-\boldsymbol{a}p/v$ and $-S_{ij}\,p_j$) in the fluid rest frame
  - Backtracking argument: The forces introduce a time reversal increment of the distribution function in the momentum space

$$\Delta f \approx -\tau\left(\boldsymbol{v}\cdot\boldsymbol{\nabla} f + \dot{\boldsymbol{p}}\cdot\partial f/\partial \boldsymbol{p}\right)$$

  - This may be referred to as an inhomogeneous CG effect

Large-Scale Anisotropies from Regular Fluid Nonuniformity

- Inertial dipole anisotropy
  - Difficulty: The CR data fit requires a fluid acceleration ~ 1-100 μm/s² ≫ the typical acceleration ~ 0.2 nm/s² in the interstellar medium (ISM)
  - Can strong nonuniformity such as shocks provide an enough acceleration?

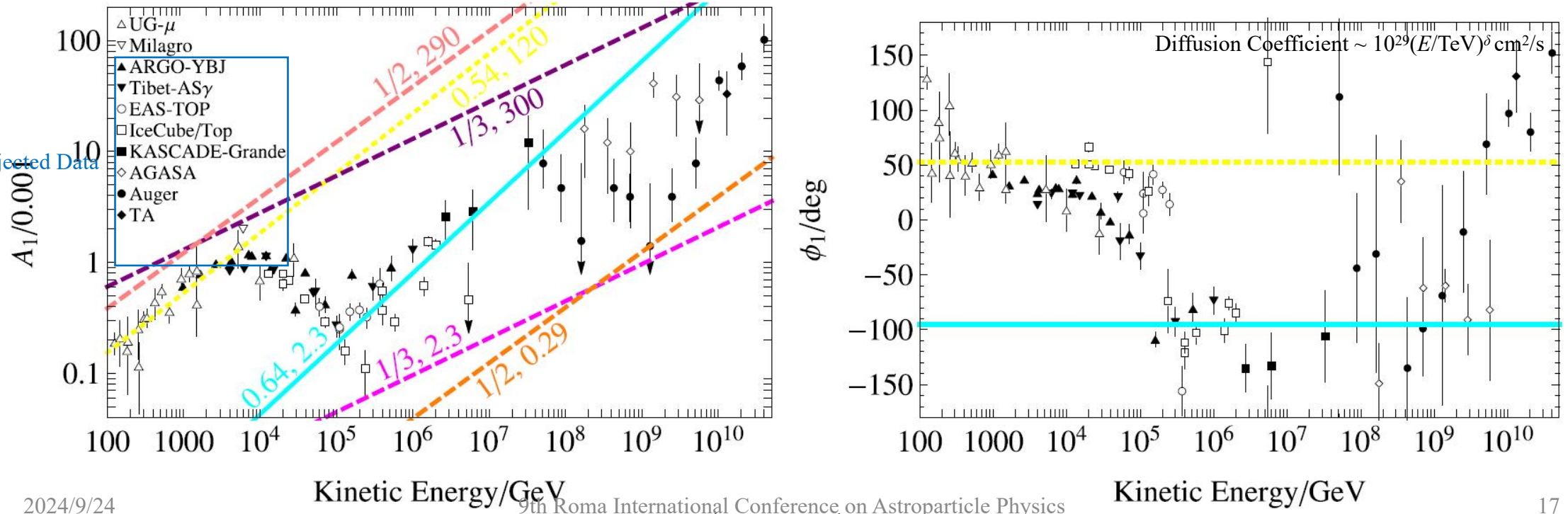

R.A. Projected Data

Zhang et al. 2022 ApJ

Large-Scale Anisotropies from Regular Fluid Nonuniformity

- Shear quadrupole anisotropy
  - The CR data fit requires a shear rate ~ 0.1-10 Myr^{-1}, which seems to be comparable with the typical ISM value
  - Anomalous second-harmonic signal in 10-100 TeV: There may be two regimes

R.A. Projected Data

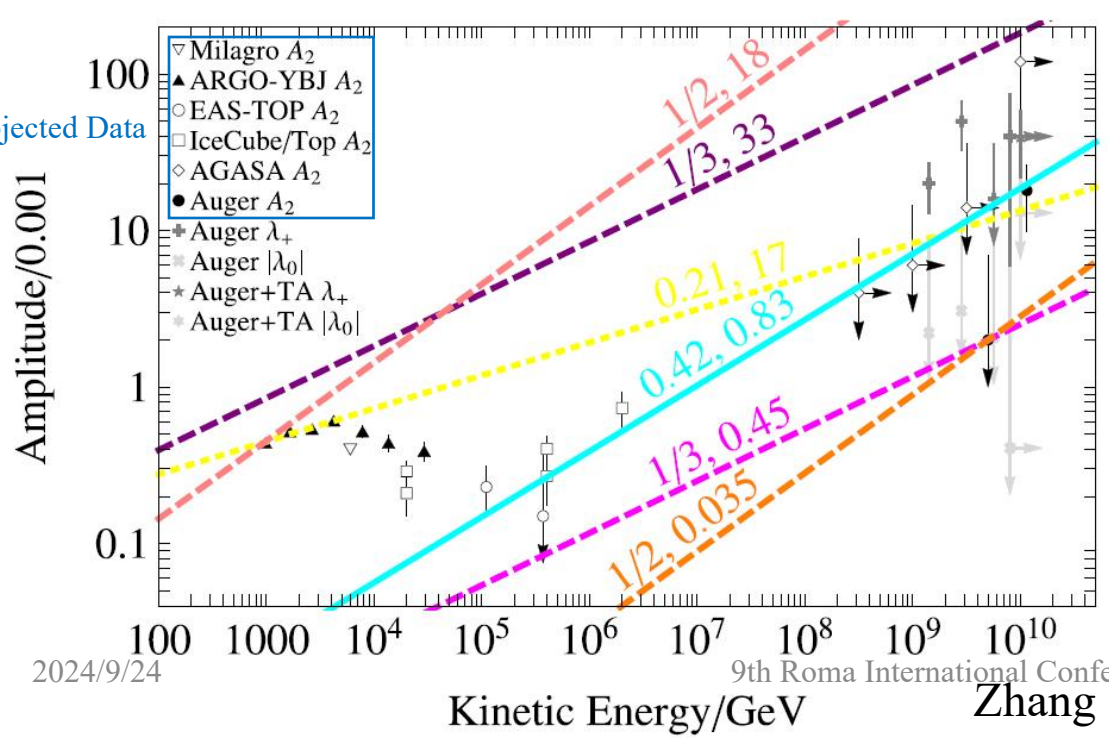

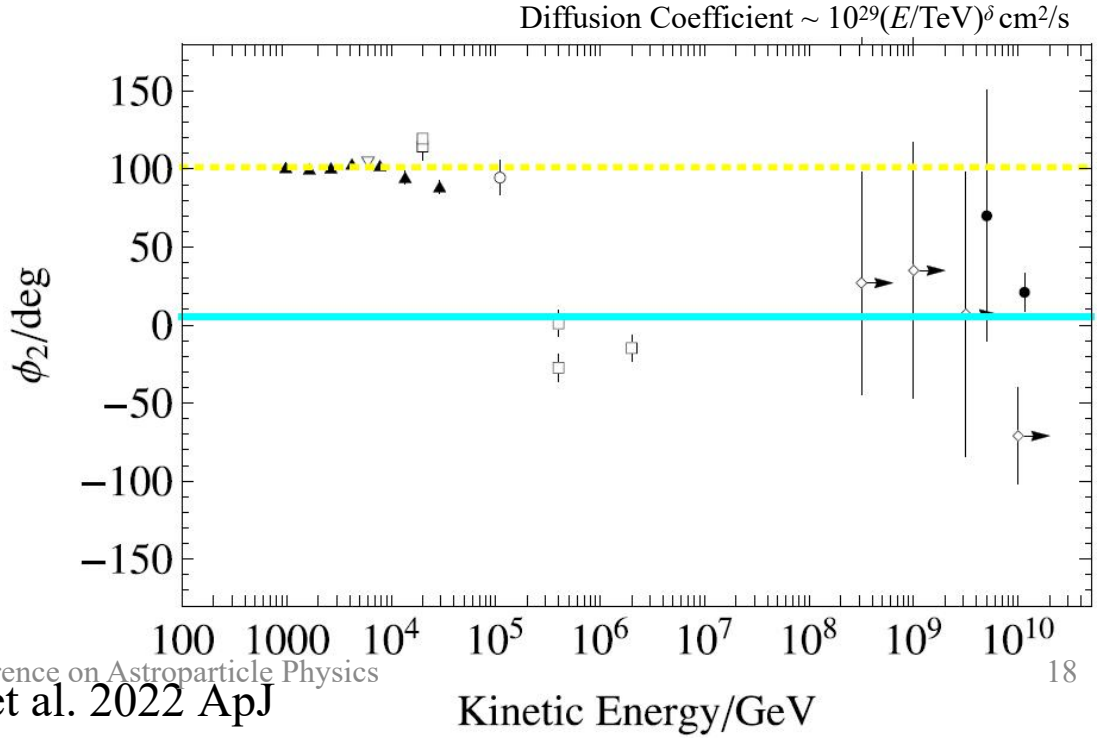

Zhang et al. 2022 ApJ

Large-Scale Anisotropies from Regular Fluid Nonuniformity

- Quadrupole anisotropy from Galactic differential rotation
  - Left: CR shear anisotropy calculated with Oort constants
  - Right: Most similar quadrupole observation to the Oort anisotropy, within large observational uncertainties

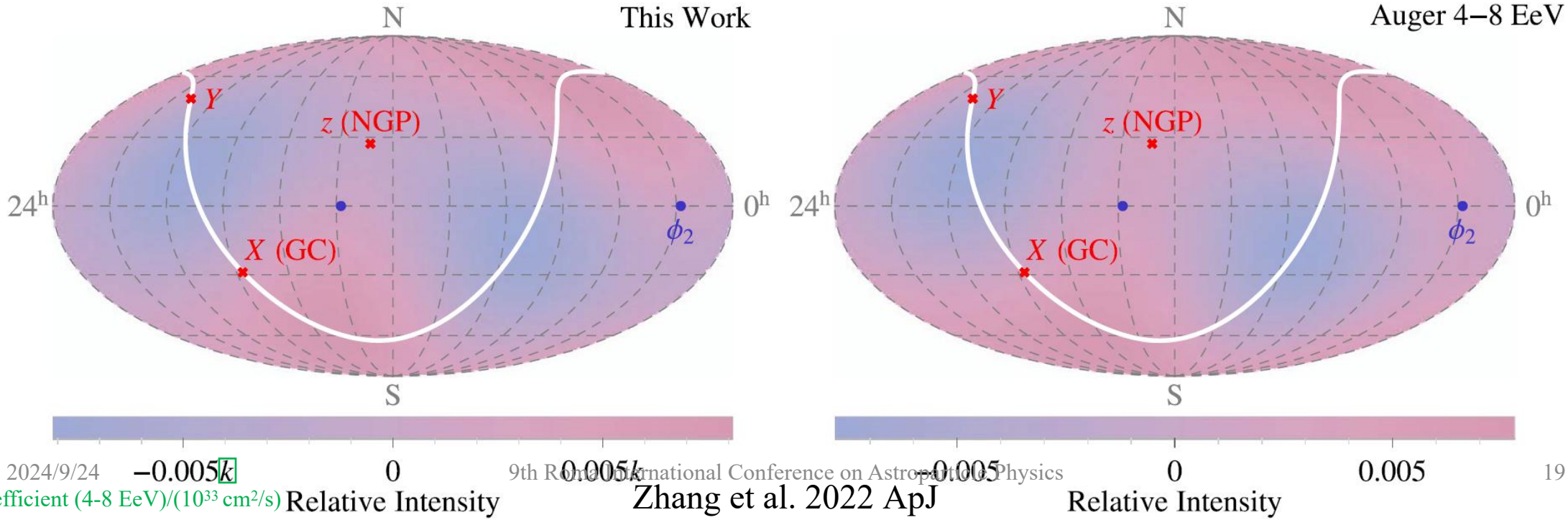

Zhang et al. 2022 ApJ

Small-Scale Anisotropies from Turbulent Convection

- Small-scale anisotropies imply the correlation of particle trajectories, which is however washed out by pure classical diffusion
- Qualitative mechanisms
  - Nondiffusive transport (Kotera 2013 PLB, Harding et al. 2016 ApJ)
  - Nonuniform pitch-angle scattering (Malkov et al. 2010 ApJ)
- Relative diffusion (Ahlers 2014 PRL, Ahlers & Mertsch 2015 ApJL, Kuhlen et al. 2022 ApJ)
  - Particles with very similar initial conditions “always” stay correlated
  - The CR angular power spectrum can be quantified with relative diffusion
- Can the nonuniform convection scenario (with the classical diffusion approximation) be extended to $\ell > 2$?

Small-Scale Anisotropies from Turbulent Convection

- Recall the (classical) convection-diffusion approximation, but now retain a finite difference of the flow velocity

$$\Delta_{\mathrm{ICG}} f = -\frac{\partial f}{\partial \boldsymbol{p}} \cdot \Delta \boldsymbol{p} = \frac{\boldsymbol{p} \cdot \Delta \boldsymbol{u}}{v} \frac{\partial f}{\partial p}$$

- The flow field can be expanded into a Taylor series $\Delta \boldsymbol{u} = \sum_l \boldsymbol{U}_{l-1}$ around $\boldsymbol{\lambda} = \boldsymbol{0}$, with $U_l \sim u\Gamma(v+1)(\lambda/\Lambda)^l \sin[\pi(v-l)]/(\pi l^{v+1})$ for $l \gg 1$ (assuming $u \propto \Lambda^v$, where Λ is the fluid scale)
  - Regular flow ($\Lambda \gg \lambda$): No small-scale anisotropy
  - Turbulence ($\Lambda \sim \lambda$): The flow varies irregularly between any two spatial points, so small-scale anisotropies can exist in many energies
  - Under relaxation ($\Lambda < \lambda$): The fluid description is invalid

Small-Scale Anisotropies from Turbulent Convection

- On the mean free path scale, the fluid of CRs has the same shape of $\Delta \boldsymbol{u}$ as that of background scattering centers, which is a superposition of the background small-scale structures
- Spherical harmonic expansion

$$\Delta \boldsymbol{u} = \sum_{L=0}^{\infty} \boldsymbol{u}_L = \sum_{L=0}^{\infty} \sum_{M=-L}^{L} \boldsymbol{c}_{LM} Y_{LM} \left(\frac{\boldsymbol{\lambda}}{\lambda} \right)$$

  - The turbulence spectrum is encoded in the Fourier expansion of the velocity correlation function
  - The Fourier description can be transformed into the spherical harmonic one via the plane wave expansion

Small-Scale Anisotropies from Turbulent Convection

- Equipartition hypothesis (for directional degrees of freedom)

$$\overline{u_L^2} = \overline{\langle u_L^2 \rangle} = (2L+1) \int_0^\infty j_L^2 (k\lambda)\, w(k)\, dk$$

  - δ-function approximation of j_L: $\overline{u_L{}^2} \sim \pi w(k_L)/(2\lambda)$, where $k_L \sim L/\lambda$
  - Geometric interpretation: The Lth structures have an effective angular scale $2\pi/L$, corresponding to two points separated by a length scale $2\pi\lambda/L$ on a sphere of radius λ, and in the interval $k_{L+1} - k_L$ the velocity variance between the two points is roughly $\overline{u_L{}^2}$

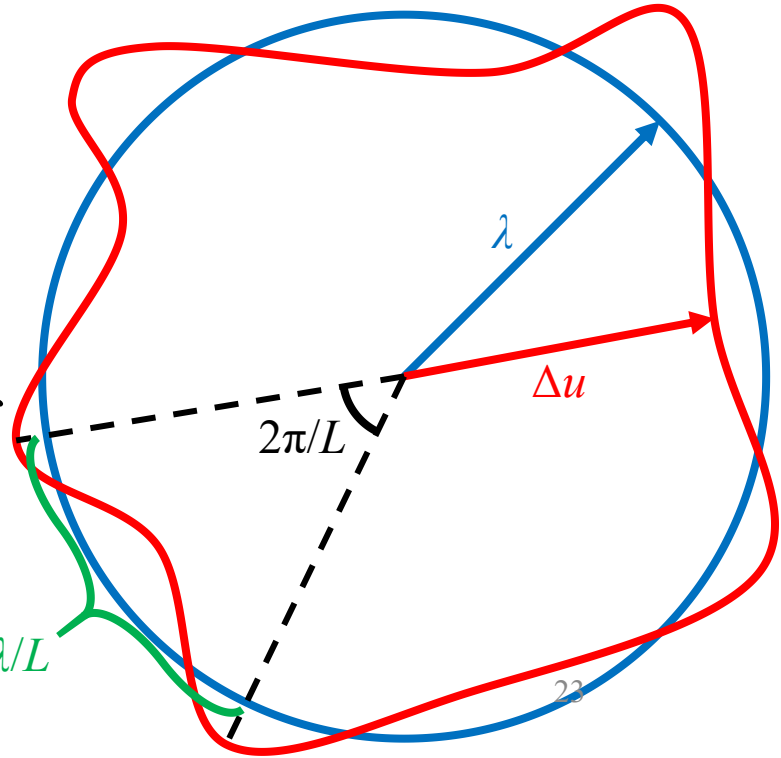

Small-Scale Anisotropies from Turbulent Convection

- The data fit at 10 TeV is consistent with the observed ISM spectrum
  - Kolmogorov law $\gamma = 5/3$
  - Velocity dispersion (10 pc) ~ 20 km/s: Alfvénic convection

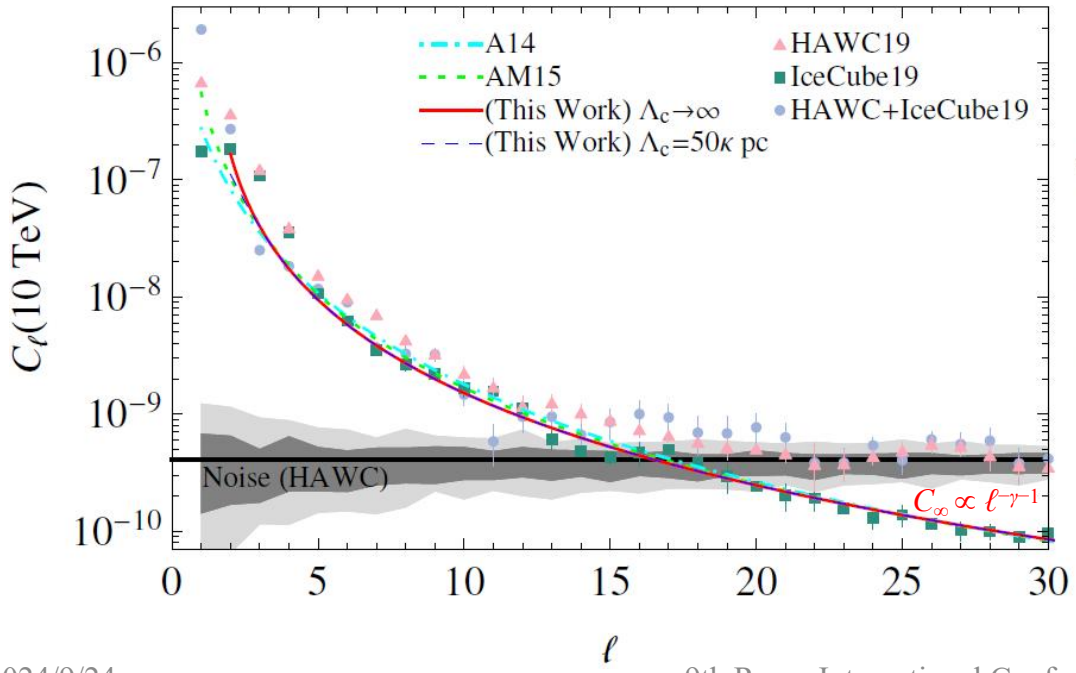

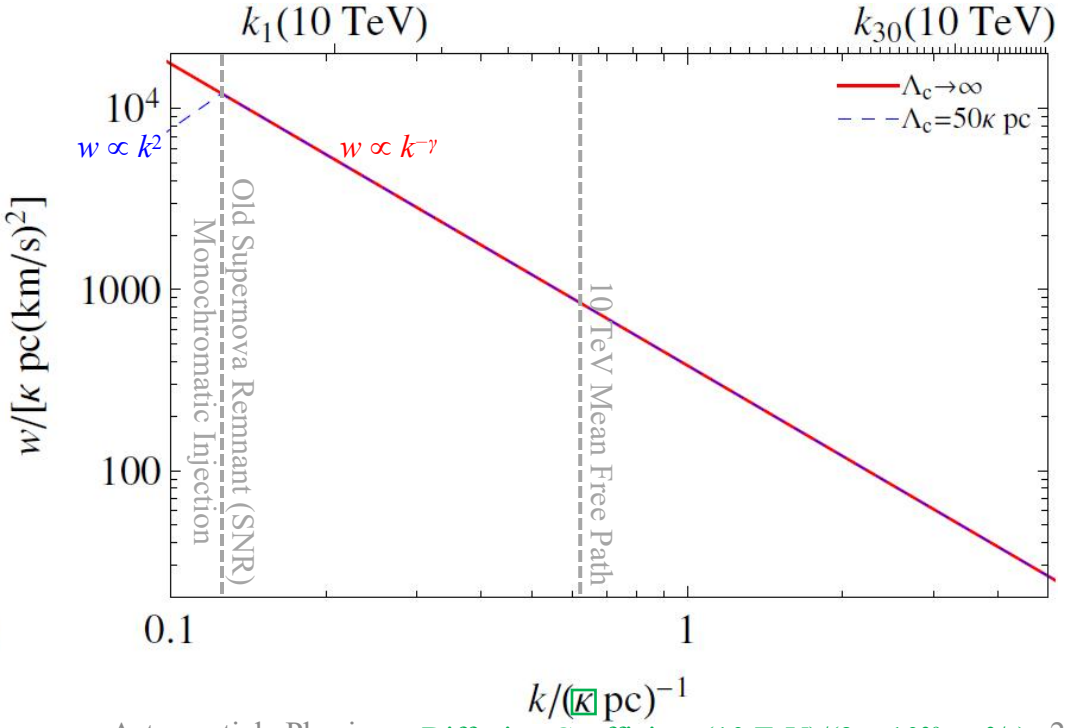

Zhang & Liu 2024 ApJL

Small-Scale Anisotropies from Turbulent Convection

- Multi-energy angular power spectra
  - Power-law turbulence spectrum & quasilinear diffusion theory: $C_\ell \propto p^{(\gamma-1)(2-\gamma_g)}$, where γ_g is the spectral index of turbulence on the gyro-resonance scale $2\pi r_g$

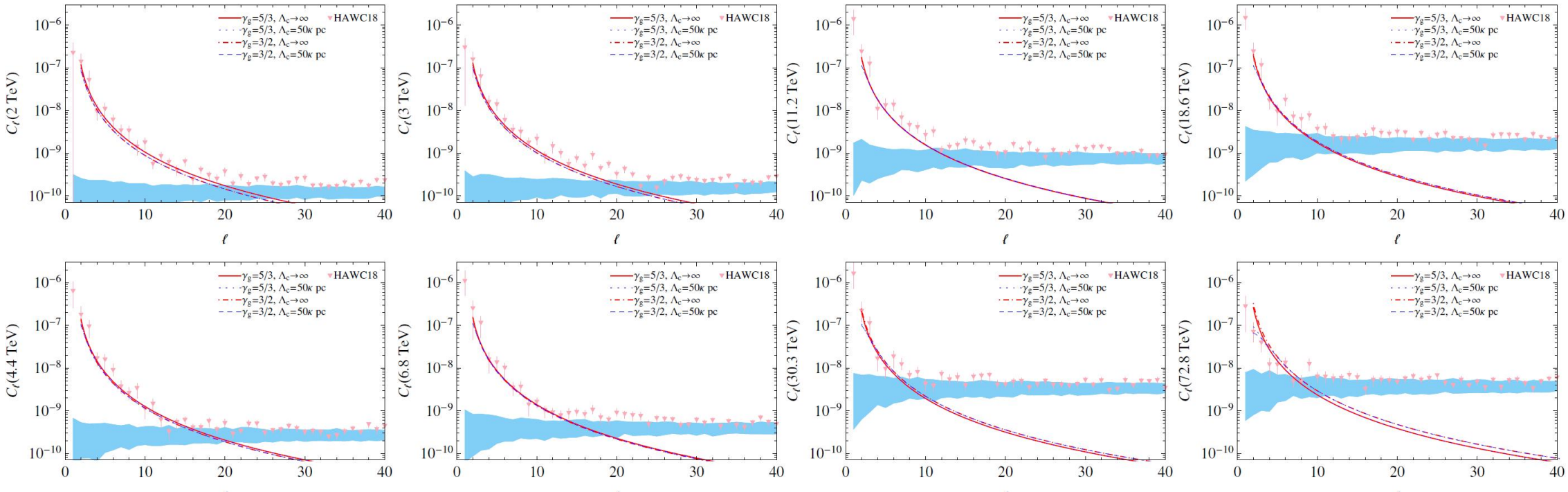

Zhang & Liu 2024 ApJL

Conclusions

With in the frame-work of classical diffusion-convection, cosmic ray spectra and anisotropy can be explained by considering the influence of local interstellar medium and the nonuniform Compton-Getting effect.

Thank you for your attention!

Small-Scale Anisotropies from Turbulent Convection

- Anomalous energy dependence of the angular power
  - There seems to be also an angular power decrease in 10-100 TeV, which cannot be explained with the SNR injection effect alone
  - A change of the turbulence spectral shape around the 10 TeV gyro-resonance scale ~ 0.02 pc?

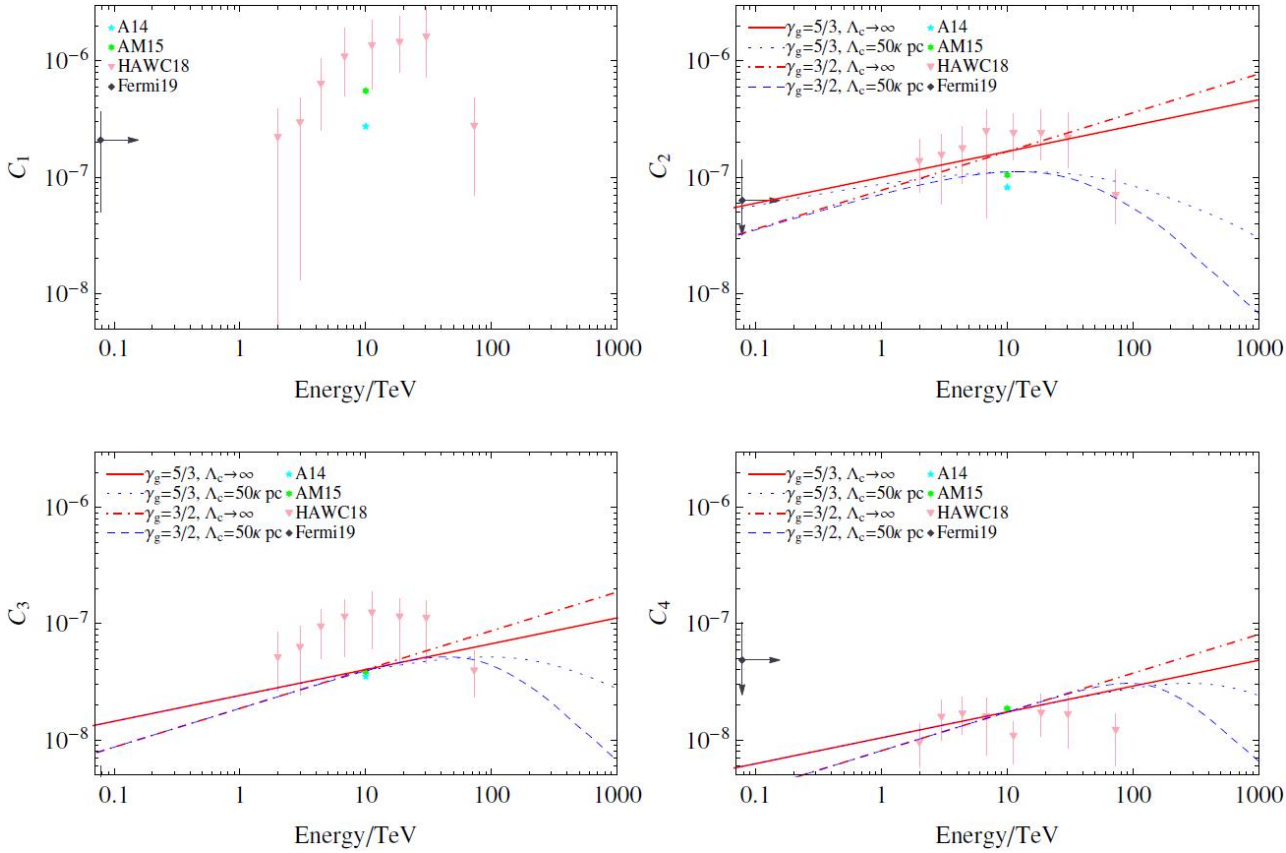

Zhang & Liu 2024 ApJL

Small-Scale Anisotropies from Turbulent Convection

- Voyager: There could be an enhancement of the turbulence power below the heliospheric bow wave scale ~ 0.01 pc

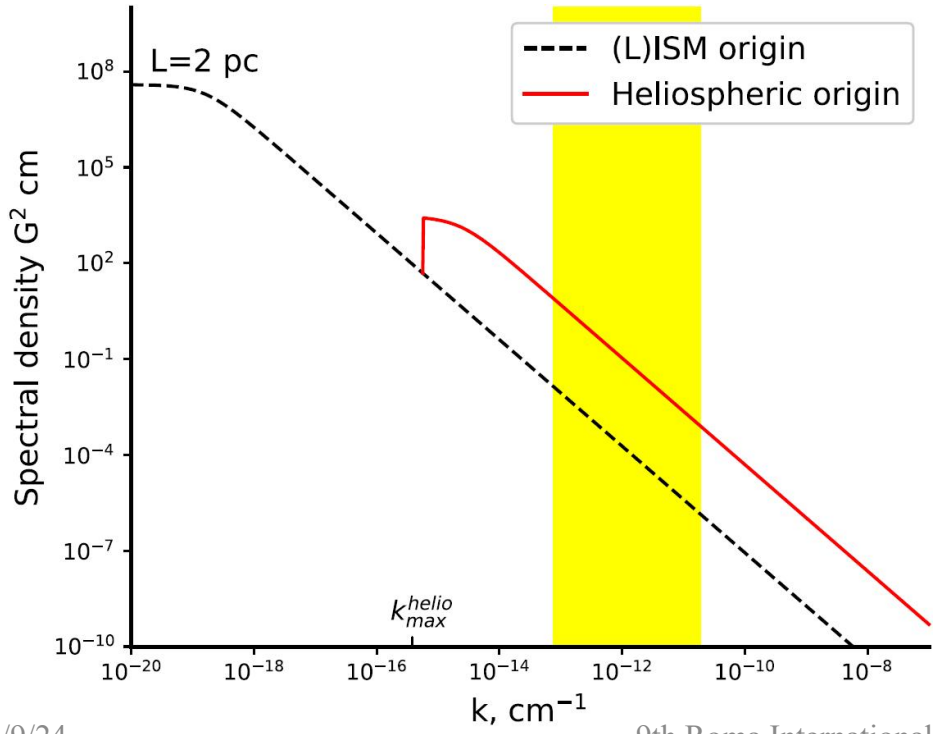

Zank et al. 2019 ApJ

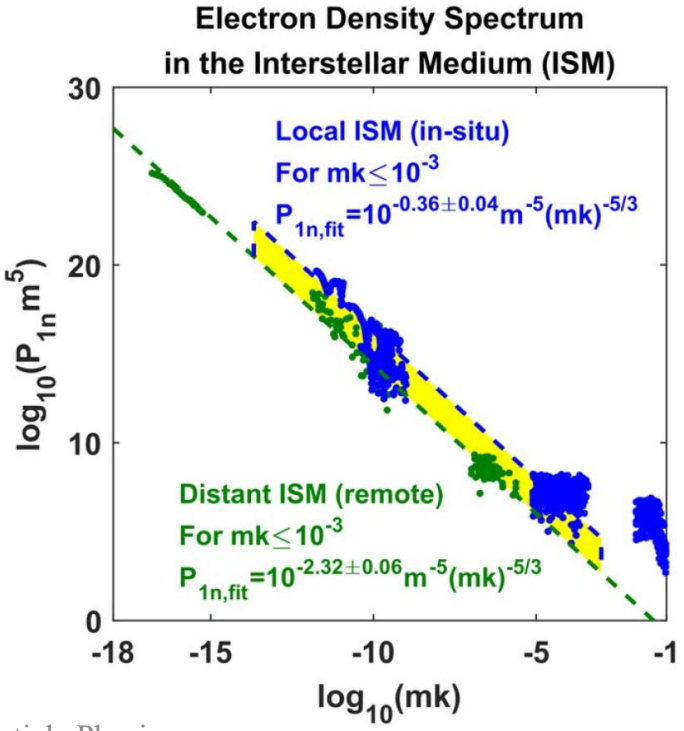

Lee & Lee 2020 ApJ

Small-Scale Anisotropies from Turbulent Convection

- Summary
  - Within the classical convection-diffusion approximation, turbulence can produce significant small-scale anisotropies in the particle distribution, with the angular power spectrum a signature of the turbulence spectrum
  - The TeV CR angular power spectrum can be described by the convection scenario approximately with the Kolmogorov law $\gamma = 5/3$ and a velocity dispersion ~ 20 km/s on the scale of 10 pc
  - The anomalous energy dependence of the angular power in 10-100 TeV remains to be investigated by future precise observations and theoretical work
  - The role of convection in the CR anisotropy problem may be more important than one conventionally expected

Large-Scale Anisotropies from Regular Fluid Nonuniformity

- Summary
  - In the classical diffusion approximation, nonuniform convection can induce dipole and quadrupole anisotropies proportional to the diffusion coefficient, via inertial and shear forces, respectively
  - The typical ISM acceleration is too small to produce the CR dipole anisotropy
  - Observations show that there is also an anomalous signal for the second-harmonic anisotropy in 10-100 TeV
  - The shear effect due to Galactic differential rotation may be important for the PeV-EeV quadrupole anisotropy
  - There is a lack of observational results for the quadrupole tensor anisotropy (instead of the 1D second-harmonic anisotropy projected on the equatorial plane); as far as we know, above 100 TeV such results have only been reported by the Pierre Auger Observatory at EeV energies

Small-Scale Anisotropies from Turbulent Convection

- The 2^ℓ-pole moment of the distributional fluctuation is determined by the coupling of dipole and (flow-velocity) 2^L-pole moments
  - Angular power spectrum

$$C_\ell = \left(\frac{1}{v}\frac{\partial \ln f}{\partial \ln p}\right)^2 \frac{1}{2\ell+1} \sum_{m=-\ell}^{\ell} \overline{|a_{\ell m}|^2}$$

$$4\pi \overline{\left\langle (\Delta_{\mathrm{ICG}} f)^2 \right\rangle} / f^2 = \sum_{\ell=0}^{\infty} (2\ell+1)\, C_\ell$$

  - The coupling result under the equipartition hypothesis

$$\overline{a_{\ell m} a^*_{\ell' m'}} = \left(A_\ell \delta_{\ell\ell'} + \mathcal{A}_{\ell m}\delta_{\ell,\ell'+2} + \mathcal{A}_{\ell' m}\delta_{\ell',\ell+2}\right)\delta_{mm'}$$

$$A_\ell = \frac{4\pi}{3\,(2\ell+1)}\left(\frac{\ell}{2\ell-1}\overline{u^2_{\ell-1}} + \frac{\ell+1}{2\ell+3}\overline{u^2_{\ell+1}}\right)$$